Compact unambiguous differential path-length metrology with dispersed Fabry-Perot laser diodes for a space interferometer array

Lagadec, T., Ireland, M., Hansen, J., Mathew, J., Travouillon, T., et al.

T. Lagadec, M. Ireland, J. Hansen, J. Mathew, T. Travouillon, S. Madden, "Compact unambiguous differential path-length metrology with dispersed Fabry-Perot laser diodes for a space interferometer array," Proc. SPIE 11446, Optical and Infrared Interferometry and Imaging VII, 114462F (13 December 2020); doi: 10.1117/12.2561927

Event: SPIE Astronomical Telescopes + Instrumentation, 2020, Online Only

Compact unambiguous differential path-length metrology with dispersed Fabry-Perot laser diodes for a space interferometer array

Lagadec T.[a], Ireland M.[a], Hansen J.[a], Mathew J.[a], Travouillon T.[a], and Madden S.[b]

[a]Research School of Astronomy and Astrophysics, Australian National University, ACT 2611, Australia
[b]Research School of Physics, Australian National University, ACT 2601, Australia

ABSTRACT

A space interferometer could reach a sensitivity and angular resolution which is unattainable on Earth due to the distortion and absorption of the atmosphere. It would enable many unique science cases, including the direct imaging and characterisation of temperate terrestrial exoplanets. This ambitious vision relies on the formation flying of individual spacecrafts, and the demonstration of precision metrology measuring positions in to better than 1mm in at least 2 dimensions, and velocities in the range of nm/s. These significant technical challenges are one of the main reasons progress in space interferometry has been seriously hampered in the two last decades. To overcome this obstacle, we propose a novel metrology concept operating in two steps. The coarse positioning of the array elements is achieved through commercially demonstrated components, such as GPS, wide angle cameras and time-of-flight sensors. For the critical fine metrology, multiple longitudinal mode Fabry-Perot lasers in a central spacecraft are split and retro-reflected off each telescope bearing spacecraft. The reflected beams are then coherently combined in the central spacecraft and the resulting fringes are spectrally dispersed. In this manner, the phase difference is measured at the different Fabry-Perot wavelengths, allowing the unambiguous differential position measurements over a couple of mm capture range. We present the concept together with a prototype system in the laboratory.

Keywords: metrology, space interferometry, formation-flying, exoplanet imaging

1. SPACE INTERFEROMETRY FOR EXO-EARTHS CHARACTERISATION

While most exoplanets discoveries have been made from indirect detections sufferring from selection biases, direct observation techniques would allow their sought after characterisation. Extreme resolution and contrast are required for this task, putting direct imaging techniques at the frontier of current instrumental capabilities. Interferometry is a good candidate for directly exoplanets. In fact, it offers high angular resolution by combining the light from telescopes separated over hundred of meters. Furthermore, a π-phase delay can be introduced into one of the interferometric arms to destructively interfere on-axis starlight, dimming the starlight and increasing the contrast of the planet/star light, a technique known as nulling interferometry.[1]

The mid-infrared region has been identified as an important window of observation for the study of young terrestrial planets. In fact, the newly formed planets shine brightly in the mid-infrared as they start to cool down. Many relevant bio-signatures are also found in this spectral region.[2] Part of these wavelengths are absorbed by the Earth's atmosphere before reaching telescopes on the ground. The atmosphere also degrade starlight at all wavelengths, severely diminishing the resolution and contrast of instruments. Lastly, ground based telescopes suffer from background radiation in the mid-infrared.

A space based interferometer would be immune from the atmospheric problems and could potentially achieve very high angular resolution and high contrast at high stability. A key technology to operate an interferometer from space is the formation flying of spacecrafts as well as an accurate and precise metrology system. Current GPS technologies have demonstrated mm precision metrology for example with the GRACE mission,[3] but

E-mail: tiphaine.lagadec@anu.edu.au

Optical and Infrared Interferometry and Imaging VII, edited by Peter G. Tuthill, Antoine Mérand, Stephanie Sallum, Proc. of SPIE Vol. 11446, 114462F · © 2020 SPIE
CCC code: 0277-786X/20/$21 · doi: 10.1117/12.2561927

interferometers requires sub wavelength (wavelength of astrophysical observation) precision in order to coherently interfere the starlight. In the late 90's, both NASA and ESA were interested in space interferometry with two key mission proposals; Terrestrial Planet Finder (TPF from NASA)[4] and Darwin (from ESA).[5] However, both missions never came to fruition due to the immature state of the formation flying metrology technologies.

There is currently a renewal of interest for space interferometry, for example with the rebooting of a Darwin-like mission as the Large Interferometer For Exoplanets (LIFE)[6] proposal for ESA's Voyage 2050 plan. Complex metrology systems will be critical to enable the formation flying of such missions. A proposed metrology architecture of several sub-systems of coarse and fine metrology is presented in this manuscript.

2. FINE METROLOGY USING COHERENT LIGHT

Coarse metrology can be achieved using GPS, wide-angle imaging cameras, and time-of-flight (TOF) sensors (fast cameras measuring the return time of retro-reflected pulsed light). These methods are readily available to measure large distances but come at the cost of low precision.

Fine metrology can be achieved using interferometry to measure relative distances at sub-wavelength precision, however absolute measurements can opnly be made for distances shorter than half of the wavelength used. For a coherent source of wavelength λ, the phase ϕ of an interferogram relates to the pathlength difference Δr between the two interferometric arms as:

$$\phi = 2\pi \left(\frac{\Delta r}{\lambda} + n \right), \tag{1}$$

with n the integer number of fringe. Unless using a time consuming technique of fringe scanning, n is not known, so that Δr can only be calculated instantaneously and unambiguously in the range $[-\frac{\lambda}{2}, \frac{\lambda}{2}]$ known as the Non Ambiguous Range (NAR). Using a longer metrology wavelength λ increases the unambiguous range but also decreases the sensitivity of the measurement.

Two wavelength interferometry[7] attempts to overcome this problem by using two different wavelengths λ_1 and $\lambda_2 > \lambda_1$ to create a synthetic wavelength Λ_{12}:

$$\Lambda_{12} = \frac{\lambda_1 \lambda_2}{\lambda_2 - \lambda_1}. \tag{2}$$

Eq. 1 can be written for each wavelength, and by subtracting one to another:

$$\phi_1 - \phi_2 = 2\pi \left(\left(\frac{1}{\lambda_1} - \frac{1}{\lambda_2} \right) \Delta r + n_1 - n_2 \right), \tag{3}$$

which simplifies to:

$$\Delta r = \Lambda_{12} \left(\frac{\phi_1 - \phi_2}{2\pi} + \Delta n_{12} \right), \tag{4}$$

with $\Delta n_{12} = n_2 - n_1$. Assuming λ_1 and λ_2 are close enough so that $\Delta n_{12} \approx 0$ an estimation of the pathlength difference $\widetilde{\Delta r_{12}}$ can be made from the measured phases $\widehat{\phi_1}$ and $\widehat{\phi_2}$:

$$\widetilde{\Delta r_{12}} = \frac{\widehat{\phi_1} - \widehat{\phi_2}}{2\pi} \Lambda_{12}. \tag{5}$$

This is used to estimate the fringe orders n_1 and n_2:

$$\widetilde{n_1} = \text{Round}\left(\frac{\widehat{\phi_1}}{2\pi} - \frac{\widetilde{\Delta r_{12}}}{\lambda_1}\right) \tag{6}$$

$$\widetilde{n_2} = \text{Round}\left(\frac{\widehat{\phi_2}}{2\pi} - \frac{\widetilde{\Delta r_{12}}}{\lambda_2}\right), \tag{7}$$

which are then used in Eq.1 to optain a better estimate of Δr. In that manner the synthetic wavelength is used to estimate the fringe order over a large NAR, and a more sensitive pathlength measurement is obtained using the estimated fringe order with the individual wavelengths. For this technique, typically the wavelengths need to be stabilised adding more instrumental complexity.

Multi wavelength interferometry is built on the principle of two wavelength interferometry, adding more wavelengths to increase even more the NAR. For example, the synthetic wavelength for a 4 wavelengths interferometer is:

$$\Lambda_{1234} = \frac{\lambda_1\lambda_2\lambda_3\lambda_4}{(\lambda_2-\lambda_1)\lambda_3\lambda_4 - (\lambda_4-\lambda_3)\lambda_1\lambda_2}. \tag{8}$$

The fine metrology proposed here uses two Fabry Perot laser diodes (FPD) of central wavelength 795 nm and 830 nm with modes spacing 0.3 nm and 0.25 nm respectivelly. Some of the resulting synthetic wavelengths are tabulated in Tab. 1 where is seen that a larger NAR of 8.95 mm can be achieved.

This range is achievable with a coarse metrology system, so that the fine metrology can provide an absolute precise measurement. In order to differentiate the different modes, the interference fringe are spectrally dispersed. All phases are therefore measured simultaneously. This removes the need for high mechanical and optical stability. Additionally, using FPD provides multiple phase measurements (Eq. 1) so that the wavelength stabilisation is not required as for the the two wavelength interferometry.

λ_1	795 nm
λ_2	795.3 nm
λ_3	830 nm
λ_4	830.25 nm
Λ_{13}	18.85 μm
Λ_{24}	17.8 μm
Λ_{12}	2.11 mm
Λ_{34}	2.76 mm
Λ_{1234}	8.95 mm

Table 1. The nomimal fine metrology FPD wavelengths with the corresponding constructed synthetic wavelengths.

3. METROLOGY IMPLEMENTATION FOR A SPACE INTERFEROMETER

3.1 Array configuration

Following the work from Hansen et al.[8] Fig.1 illustrates a possible single baseline space interferometer configation. Two 'deputy' satellites form the interferometric array. Each satellite carries a telescope reflecting the starlight to a central 'chief' satellite which performs the science beam combinationas well as the metrology. All satellites are equipped with their own star tracker to align to the astrophysical target.

Using the central satellite as reference, the optical path difference (opd) between deputy 1 and deputy 2 is:

$$opd = |d_1| - d_1.\vec{s} - |d_2| + d_2.\vec{s}, \tag{9}$$

as shown in Fig. 1.

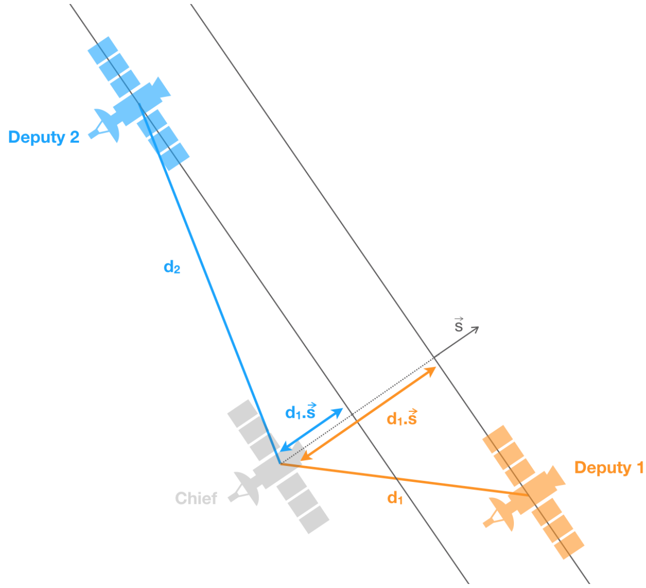

Figure 1. Illustration of a single baseline space interferometer array. Two 'deputy' satellites form the interferometric array. The light between the two deputies is sent off to a central 'chief' satellite that performs the beam combination as well as other operational tasks such as the metrology. The optical path difference between the two deputy needs to be measured and compensated for. In this illustration the distances are exaggerated for clarity.

Fig. 2 depicts the metrology geometry from the chief to the deputies. One retro-reflector is centrally positioned on each deputy. Inside the chief, the light from the two modulated FPD is split into 4 beams at A, B, C, D, and each are retro reflected onto the deputies back into the chief along d_a, d_b, d_c and d_d forming 4 laser links. This allows for more degrees of freedom to be measured.

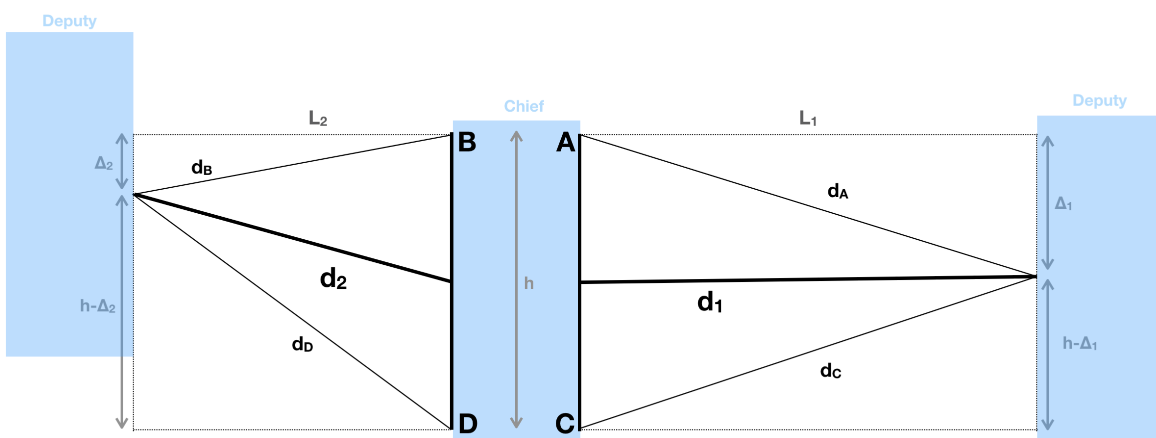

Figure 2. Metrology architecture. The metrology light is split into 4 outputs at A, B, C and D. The outputs are retro-reflected on the deputies into the chief providing 4 laser links d_a, d_b, d_c and d_d to measure d_1 and d_2 in two dimensions.

Using trigonometry:

$$\Delta_1 = \frac{d_A^2 - d_C^2}{2h} + \frac{h}{2}, \tag{10}$$

and

$$d_1 = \frac{1}{2}\sqrt{(d_A + d_C)^2 + (d_A - d_C)^2 - h^2}. \tag{11}$$

Assuming $h << d_1$ and performing a Taylor expansion at $d_A - d_c \to 0$:

$$d_1 \approx \frac{1}{2}\sqrt{(d_A + d_C)^2 - h^2} + \frac{(d_A - d_C)^2}{4\sqrt{(d_A + d_C)^2 - h^2}}. \tag{12}$$

$\sqrt{(d_A + d_C)^2 - h^2}$ is rewritten as:

$$\sqrt{(d_A + d_C)^2 - h^2} = (d_A + d_C)\sqrt{1 - \left(\frac{h}{d_A + d_C}\right)^2} \tag{13}$$

Which can be further simplified by performing a new Taylor expansion:

$$\sqrt{1 - \left(\frac{h}{d_A + d_C}\right)^2} \approx 1 - \frac{1}{2}\left(\frac{h}{d_A + d_C}\right)^2, \tag{14}$$

giving:

$$\sqrt{(d_A + d_C)^2 - h^2} \approx (d_A + d_C)\left(1 - \frac{h^2}{2(d_A + d_C)^2}\right) \tag{15}$$

Finally

$$d_1 \approx \frac{d_A + d_C}{2}\left(1 - \frac{h^2}{2(d_A + d_C)^2}\right) + \frac{(d_A - d_C)^2}{4(d_A + d_C)}. \tag{16}$$

$$\tag{17}$$

The same reasoning is applied for d_2 leading to

$$d_1 - d_2 = \frac{d_A + d_C - d_B - d_D}{2} - \frac{h^2}{4(d_A + d_C)} + \frac{h^2}{4(d_B + d_D)} + \frac{(d_A - d_C)^2}{4(d_A + d_C) - \frac{2h^2}{d_A + d_C}} - \frac{(d_B - d_D)^2}{4(d_B + d_D) - \frac{2h^2}{d_B + d_D}}. \tag{18}$$

Re-written as,

$$d_1 - d_2 = \frac{1}{4}\left(1 - \frac{h^2}{8\bar{d}^2}\right)(\Delta_{AB} + \Delta_{AD} + \Delta_{CB} + \Delta_{CD}) + \frac{1}{8\bar{d}}\left(\Delta_{AC}^2 - \Delta_{BD}^2\right), \tag{19}$$

with $\bar{d} = \frac{1}{4}(d_A + d_B + d_C + d_D)$ and $\Delta_{ij} = d_i - d_j$, for readability.

The Δ values are measured with the fine metrology, and the $\bar{d}$ is measured with the coarse metrology. With $h = 0.3\,\mathrm{m}$, $\bar{d} = 5\,\mathrm{m}$ (the smallest useful space interferometer), and the Δ values within an optimistic $1\,\mathrm{cm}$ capture range, this equation is accurate to within $1.5\,\mathrm{nm}$, which is well within what is required.

3.2 Photonic technology for a compact metrology system

The metrology system is designed around a photonic chip. The chip is fabricated using the direct-write technique which uses a high repetition pulsed laser to locally and permanently modify the refractive index inside a glass substrate producing imbedded 3D waveguides. Complex waveguide circuits can be fabricated in that manner that are robust, thermally and mechanically insulated (more stable than their bulk optics conterparts) and very compact. Fig. 3 illustrates the design which dimensions are compatible with a 1U cubsat pathfinder or a larger space array. The footprint of the photonic chip with it's auxiliary components is shown in contrast to the dimensions of a 1U cubesat. Two FPD's (outside of the plane) are modulated and fiber injected into the chip through a v-groove (left top corner). The light from the two FPD's is combined through a directional coupler (first waveguide device inside the top left corner of chip), and then split into 4 outputs (right side in green). Another v-groove picks up the outputs into loose fibers, directed at the A, B, C and D exit of the chief satellite (from Fig. 2). From there the beams are retro-reflected off the deputy satellites, and re-injected into the fiber, v-groove and chip. Inside the chip, the waveguides are then split twice (green to purple and purple to blue). The different colours of the waveguides represents the waveguides being in different planes so that there is no cross talk between the waveguides. The blue path goes towards 4 photodiodes directly mounted on the chip to perform the TOF coarse metrology. The purple path brings the 4 beams to a butt-coupled planar chip, where the outputs propagate freely in one direction, so that the beams interfere at the output facet. A free-space spectrographic back ends (in another plane) will then disperse the resulting fringe on a final sensor to perform the multi-wavelength coherent metrology. In this fashion the coarse and fine metrology are performed simultaneously removing the need for very high temporal stability.

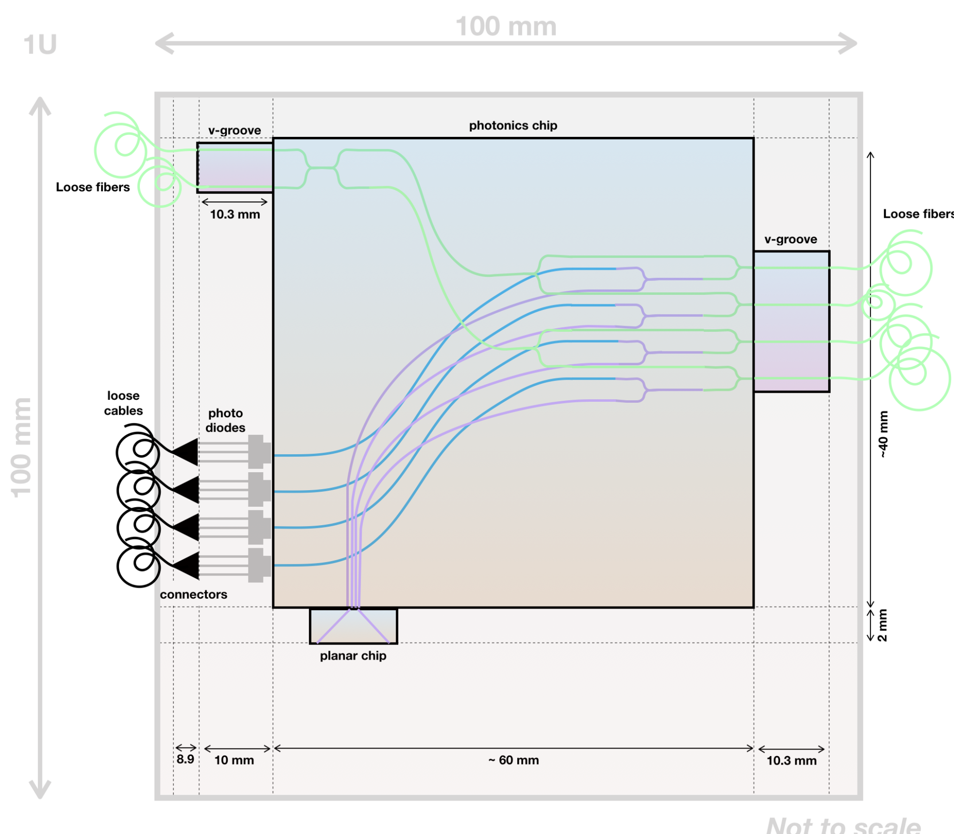

Figure 3. Illustration of the photonic chip with it's adjacent components fitting in a 1U cubSat. The dimensions of the chip, auxiliariy components and cubeSat are to scale, but the waveguides dimensions have been exagerated. The system is described in the text.

4. TWO BEAMS FINE METROLOGY LABORATORY PROTOTYPE

A laboratory experiment of a two beams system is being developed. The main goals are to characterise the contribution of spurious reflections to the metrology signals, characterise the FPD spectral response to the applied power and demonstrate the absolute metrology of two distances.

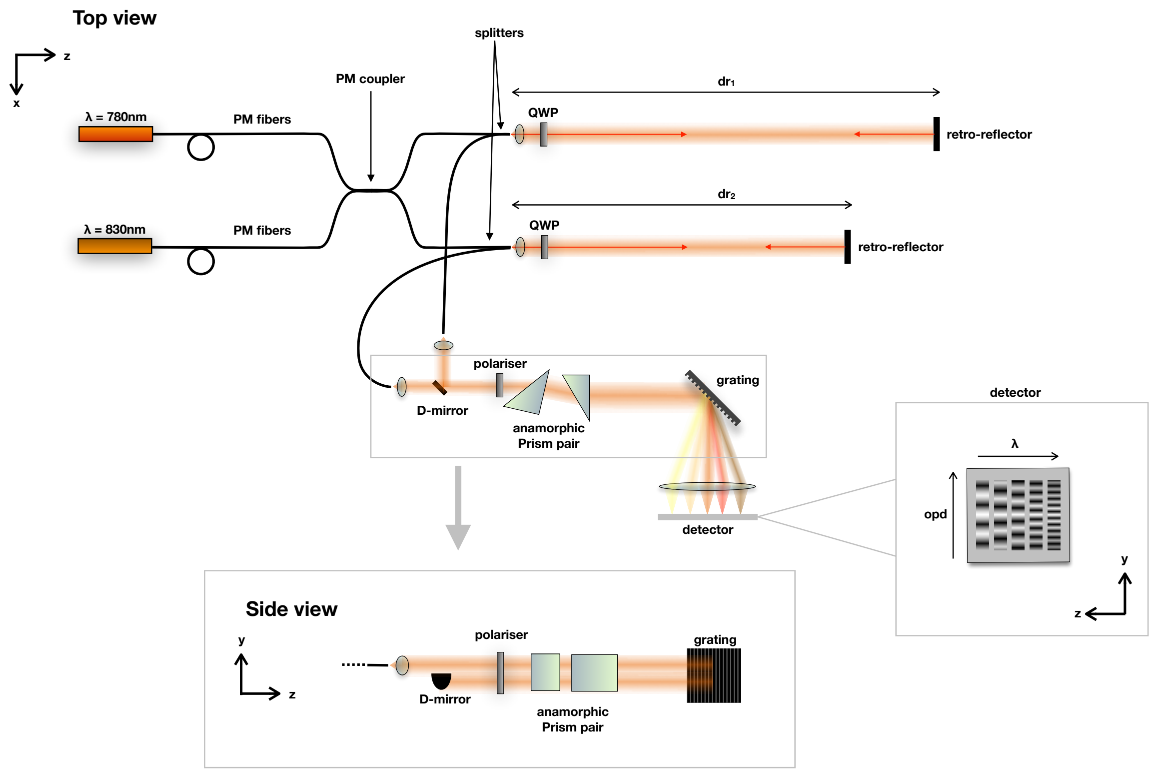

Figure 4. Schematic for the fine metrology laboratory experiment. Two FPD of $\lambda_1 = 730$ nm and $\lambda_2 = 830$ nm feed two polarisation maintaining fibers and are coupled in a 2x2 coupler. The outputs are collimated and travel two distances d_A and d_B to be measured and are reflected back with adjustable retro reflectors. The reflected beam are re-injected into fibers and recollimated one of the beams is reflected with a D-mirror in order to position both beams next to each others. A polariser is used in conjunction with the quarter wave plates (in d_A and d_B) to discriminate in polarisation the beams coming from the retro-reflectors from that coming from potential back reflections in the system. The resulting two beams go through an anamorphic prism pair that elongate the beams in one direction. They then hit a grating, and their wavelength components are collected and focussed on a detector, so that the two beams interfere and their fringe are recorded vertically and the spectrally dispersed horizontally.

The setup is displayed in Fig. 4. The two FPD are fed into polarisation maintenain (PM) fibers onto a fiber coupler where they are superposed and then split 50/50. The outputs are fed into two PM fiber splitters with one outputs being collimated and reflected onto retro-reflectors. The retro-reflectors can be moved along the optical path to change the pathlength difference. The reflected beams traverse quarter wave plates (QWP) that are rotated to remove any unwanted spurious reflections from the fiber end faces. The beams are re-injected into the splitters which sends the beams to two collimaters. A D-mirror is used to bring the two beams on top of each others (in the y-direction). A polariser is used to increase the contrast of the fringe. The beams then go through an anamorphic prism to elongate the beams horizontally (x-direction). A grating disperse the different modes of the FPD which are then focussed on a detector where the beams interfere. The detector records the spectrally dispersed fringe.

5. CONCLUSION

Formation flying of a space interferometer will require complex metrology systems to precisely measure the position of the spacecrafts over large distances. Once the distances have been measured accurately, they can be compensated for it with micro-thrusters on the spacecrafts and delay lines inside the science beam combiner.

The coarse metrology can be achieved by GPS, wide angle cameras and TOF sensors. For the fine metrology, two laser links per satellite are needed to measure positions in 2D. FPD allow to increase the NAR through the creation of synthetic wavelengths. The proposed architecture uses a photonic chip to simlutaneously produce the coarse time-of-flight metrology and the fine metrology. A laboratory experiment is being developed to test the FPD fine metrology as a first step towards a full scale space mission. A robotic ground based prototype array will follow to show the metrology of a one baseline interferometer Following, a ground based robotic array of 1 baseline with 6 degrees of freedom called Pyxis will implement the metrology with the photonics chip to observe real astrophysical target. It is hoped to then have CubeSat demonstrator of same size of the ground based pathfinder.

A pathway for a space interferometer imcludes first a laboratory demonstration for a two beams interferometer. A ground based robotic array Pyxis will then be constructed to simulate a space array, with several degrees of freedom. Finally we hope to implement and demonstrate the technology with a CubeSat array.

ACKNOWLEDGMENTS

The authors pay their respect to the traditional and rightful custodians of the land on which this project takes place: the Ngunnawal people. We recognise their sacred nurturing connection to the land and the unjust and violent dispossession they suffered and continue to face through the settler colony. We extend our respect to all First Nation people, their continuing resilience, culture and contribution.

This research was supported by the Australian Government through the Australian Research Council's Discovery Projects funding scheme (project DP200102383), and by the Australian National University through the Futures scheme.

REFERENCES

[1] Bracewell, R. N., "Detecting nonsolar planets by spinning infrared interferometer," *nat* **274**, 780 (Aug. 1978).

[2] Traub, W. A., Jucks, K. W., and Noecker, C., "Biomarkers on Extrasolar Terrestrial Planets: Estimates of Detectability," in [*American Astronomical Society Meeting Abstracts*], *Bulletin of the American Astronomical Society* **32**, 1485 (Dec. 2000).

[3] Kroes, R., Montenbruck, O., Bertiger, W., and Visser, P., "Precise grace baseline determination using gps," *GPS Solutions* **9**(1), 21–31 (2005).

[4] Beichman, C. A., Woolf, N. J., and Lindensmith, C. A., [*The Terrestrial Planet Finder (TPF) : a NASA Origins Program to search for habitable planets*] (1999).

[5] Léger, A., Mariotti, J., Mennesson, B., Ollivier, M., Puget, J., Rouan, D., and Schneider, J., "Could we search for primitive life on extrasolar planets in the near future?," *Icarus* **123**(2), 249 – 255 (1996).

[6] Quanz, S. P., Kammerer, J., Defrère, D., Absil, O., Glauser, A. M., and Kitzmann, D., "Exoplanet science with a space-based mid-infrared nulling interferometer," in [*Optical and Infrared Interferometry and Imaging VI*], *Society of Photo-Optical Instrumentation Engineers (SPIE) Conference Series* **10701**, 107011I (July 2018).

[7] Polhemus, C., "Two-wavelength interferometry," **12**, 2071.

[8] Hansen, J. T. and Ireland, M. J., "A linear formation-flying astronomical interferometer in low earth orbit," *Publications of the Astronomical Society of Australia* **37**, e019 (2020).